 DOI: 10.1002/masy.201100031

Model to Design Multilayer Tissue Engineering Scaffolds

Bernke J. Papenburg,[1] Gustavo A. Higuera,[2] Ida-Jacoba de Vries,[1] Jan de Boer,[2] Clemens A. van Blitterswijk,[2] Matthias Wessling,[1] Dimitrios Stamatialis[1,3]*

Summary: In tissue engineering scaffolds, nutrient transport to cells is a major hurdle for building viable 3D tissue scaffolds. *In vivo*, a complex network of blood vessels and capillaries delivers nutrients and oxygen to the tissue. For *in vitro* build constructs the distance to the main nutrient source is often long resulting in nutrient gradients over the scaffold and decreased cell proliferation or even cell death in parts of the scaffold. This work describes a numerical model for designing a multilayer scaffold for tissue engineering by stacking sheets featuring microchannels. These sheets fabricated by phase separation micromolding (PSμM) allow nutrient perfusion through the 3D scaffold whereas inner-porosity of the sheets guarantees diffusion between layers. The model predicts significant nutrient limitation occurs under static conditions for scaffolds having over 3 sheets. The situation can improve dramatically under dynamic conditions when perfusion occurs through the microchannels.

Keywords: micropattern; modelling; nutrient transport; scaffold; tissue engineering

Introduction

Tissue engineering (TE) aims at producing a living substitute that restores, maintains or improves the function of tissues or organs.[1] Often in TE, a matrix or scaffold provides cells a physical means for attachment. The cells attach and deposit their extra-cellular matrix (ECM) to replace a degradable scaffold in time.

In vivo, nutrient transport across tissue by pure diffusion is limited to a distance of about 200 μm from a vascular network capillary. During *in vitro* culture, cells on the scaffold obtain nutrients from surrounding culture medium. For most *in vitro* build scaffolds, distance to the main nutrient source mostly exceeds 200 μm.[2–4] Hence, during culture of constructs of clinically relevant sizes nutrient limitation is likely to occur.[4,5] Waste products, such as lactate, accumulate within these constructs causing pH decrease which in turn inhibits the ECM formation by the cells.[6–8] To reduce these limitations during culture of tissue engineered constructs, there has been considerable interest in the development of TE bioreactors that introduce convective medium flow *in vitro* to the 3D tissue scaffolds.[8–14] Previous works described a novel concept of preparing 3D-scaffolds by stacking or rolling micropatterned sheets (see Figure 1).[15,16]

Micro-channels, in the range of hundreds of microns; allow nutrient perfusion through the scaffold, provide space for cells to grow, and topography for cell organization. The sheet inner-porosity in the range of ~10 μm facilitates nutrient transport and communication between the layers. This paper presents modeling the nutrient

[1] Membrane Science and Technology group, MIRA Institute for Biomedical Engineering and Technical Medicine, University of Twente, P.O. Box 217, 7500 AE, Enschede, The Netherlands
E-mail: d.stamatialis@utwente.nl
[2] Department of Tissue Regeneration, MIRA Institute for Biomedical Engineering and Technical Medicine, University of Twente, P.O. Box 217, 7500 AE, Enschede, The Netherlands
[3] Present address: Department of Biomaterials Science and Technology, Faculty of Science and Technology, MIRA Institute for Biomedical Engineering and Technical Medicine, University of Twente, P.O. Box 217, 7500 AE, Enschede, The Netherlands

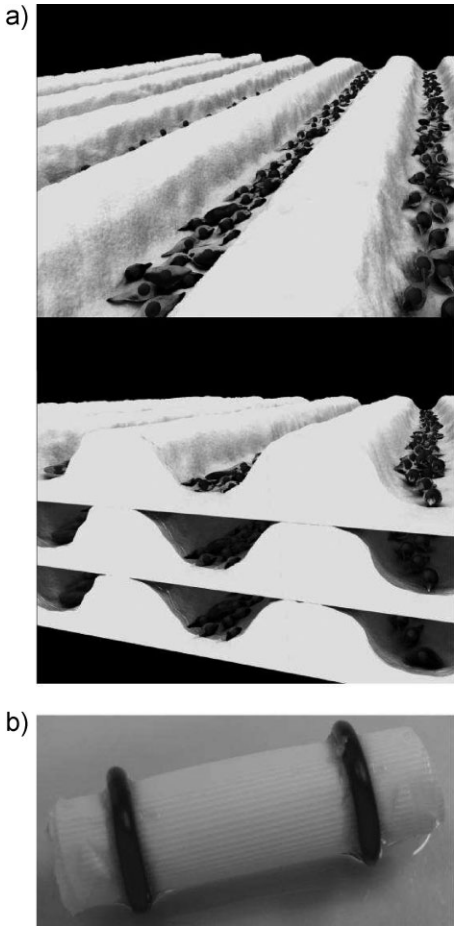

Figure 1.
(a) Illustration of multi-layer stacking; cells cultured on micropatterned sheets which are subsequently multi-layer stacked for the microchannels to provide space for cells to grow(Adapted from [15,17]); (b) Multi-layer scaffolds featuring 250 μm channels (adapted from [15]).

supply through these multilayer scaffolds. The model, developed using COMSOL multiphysics 3.3 modeling software (COMSOL 2007), predicts oxygen and glucose supply through the multi-layer scaffolds and can be used as a tool to design and construct relevant sized scaffolds using this novel concept. The modeling results are compared to cell culturing experiments under static and dynamic conditions published recently.[15]

Model Description

Figure 2 illustrates the multilayer construct and the topography dimensions the model is based on. The construct can be prepared by either stacking or by rolling the sheets. Nutrient transport through the channels is assumed not to be affected by sheet curvature due to rolling.

Model Boundaries

The designed model is general and not specified to e.g. cell type, - age, - dimension or - shape but high mean constant metabolic rates are chosen for oxygen and glucose consumption, similar to models described before.[18–21] Temperature and cell culture medium pH are considered constant since the incubator environment, the humid 5% CO_2 atmosphere combined with the medium buffer capacity control these parameters, respectively. Additional assumptions are: all processes are isothermal, cell culture medium is cell free and cells are distributed homogeneously in the microchannels. Change in cell number due to proliferation is taken into account by solving the model for two different cell densities; a lower value comparable to initial seeding density and a higher value representing higher cell confluence. These calculations allow simultaneous estimation of glucose and oxygen profile changes in time; initial values, after cell seeding and later upon cell confluence are reached.

This model assumes no change in cell culture medium density, no cell differentiation and cell death, no influence of oxygen consumption on the glucose concentration and vice versa (oxygen and glucose consumption are calculated independently) and no scaffold degradation (change in permeability is expressed by differences in diffusion coefficients obtained experimentally).

Parameters

Table 1 lists default parameter values taken from literature or determined experimentally.

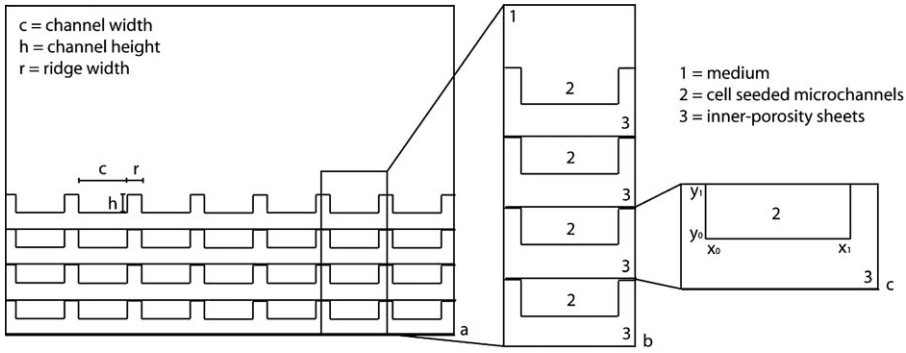

Figure 2.
Schematic illustration of multi-layer stacked sheets geometry; (a) 4 layers stacked in a well, (b) basic model geometry in static culturing, number of sheets can be adjusted (c) one symmetry element as described in the model for dynamic culturing condition. Values for channel width, height and ridge width used in this model are 250 μm, 45 μm and 40 μm respectively and total height of one symmetry element 90 μm, i.e. one sheet layer. 1–3 indicate the various domains that are distinguished in the model. During dynamic culture, medium is transported through channels (domain 2) and permeates through sheet inner-porosity (domain 3).

Static Culturing

1 ml medium per cm^2 surface area is present on top of the multi-layer scaffolds and is refreshed every 2 days, similar to the experiments. Based on symmetry of the multi-layer scaffold in width and length, the model can be solved in 2D.

Nutrient transport is based on diffusion only; therefore Fick's law is used to describe the static case:

$$\frac{\partial c}{\partial t} = \nabla \cdot (-D \nabla c) \quad (1)$$

Where c = nutrient concentration, t = time and D = nutrient diffusion coefficient; the

Table 1.
Default parameter values used in the model

	Parameter	Value	Unit	Ref[e]
General	Cell seeding density[a]	$2 \cdot 10^{12}$	cells/m^3	exp., [16,21]
	Increased cell density	$3 \cdot 10^{13}$	cells/m^3	exp., [21]
	Porosity inner-part sheets	75	%	exp., [16]
	Length microchannels	0.03	m	[21], exp. relevant
	Inlet velocity	$7.5 \cdot 10^{-3}$	m/s	[21]
Glucose	Inlet concentration[b]	5.55	mol/m^3	exp.
	D_1[c]	$9 \cdot 10^{-10}$	m^2/s	[20,22]
	D_2	$1.8 \cdot 10^{-10}$	m^2/s	[21]
	D_3	$1 \cdot 10^{-10}$	m^2/s	exp., [16,21]
	Cell metabolic rate	$3.83 \cdot 10^{-16}$	mol/(cell · s)	[21]
Oxygen	Inlet concentration[b]	0.2	mol/m^3	[8,21]
	D_1[c]	$3 \cdot 10^{-9}$	m^2/s	[20,21,23]
	D_2	$6 \cdot 10^{-10}$	m^2/s	[21]
	D_3	$3 \cdot 10^{-10}$	m^2/s	Calculated[d], [21]
	Cell metabolic rate	$3.75 \cdot 10^{-17}$	mol/(cell · s)	[20,21,24]

Dx indicates diffusion coefficient at domain x (1 = medium, 2 = cell-seeded microchannel, 3 = inner-porosity of the scaffold sheets
[a]Based on a cell seeding density of 15.000 cells/cm^2 as used in the culture experiments.
[b]Based on the glucose concentration in culture medium or blood and oxygen solubility of oxygen in water of 37 °C in an environment of 5% CO_2 respectively.
[c]Based on the diffusion coefficient of glucose/oxygen in water at 37 °C.
[d]Experimentally determined glucose diffusion coefficient through the scaffold sheet after which the oxygen diffusion coefficient has been calculated using the same ratio between D_1 and D_3 as for glucose.
[e]'exp.' stands for 'experimentally determined'.

term $(-D\nabla c)$ describes Fick's law for diffusive transport. This model assumes no interaction between glucose and oxygen transport and therefore Fick's law is applied separately for the two components.

Symmetry applies and the following general boundary conditions are applied:

$$\left(\frac{\partial c}{\partial x}+\frac{\partial c}{\partial y}\right)=0 \tag{2}$$

Describing zero flux over surfaces of symmetry.

$$D_A\left(\frac{\partial c}{\partial x}+\frac{\partial c}{\partial y}\right)=D_B\left(\frac{\partial c}{\partial x}+\frac{\partial c}{\partial y}\right) \tag{3}$$

Describing flux continuity over boundaries between domains with different diffusion coefficients.

$$c(t_0)=c_0 \tag{4}$$

Equating initial nutrient concentration conditions in the medium at the start of the experiment.

Three domains can be distinguished in static culture: cell culture medium, cell seeded microchannels and inner-porosity of the scaffold sheets. To solve the model, these three domains were considered separately with respect to equations, boundary- and initial conditions.

Cell Culture Medium in Microchannels (Domain 1)

$$\frac{\partial c}{\partial t}=D_1\left(\frac{\partial c}{\partial x}+\frac{\partial c}{\partial y}\right) \tag{5}$$

Boundary and initial conditions are described as follows:

- equation 2 is valid at the top boundary and at all exterior boundaries for glucose; representing no glucose flux between the medium-air boundary and at the sides of the stacked multi-layer scaffold sheets respectively
- at the top boundary $c=c_0$ can be applied for oxygen; describing solubility of oxygen from the air into the medium
- equation 3 is valid at the boundary between medium and microchannels when $D_A=D_1$ and $D_B=D_2$ and for the boundary between medium and inner-porosity of the sheets when $D_A=D_1$ and $D_B=D_3$; describing flux continuity over the respective boundaries
- equation 4 is valid as initial conditions; representing nutrient concentrations of fresh medium.

Cell Seeded Microchannels (Domain 2)

$$\frac{\partial c}{\partial t}-D_2\left(\frac{\partial c}{\partial x}+\frac{\partial c}{\partial y}\right)=R=V\cdot d \tag{6}$$

with V = consumption rate per cell and d = cell seeding density, multiplied V and d express zero-order consumption rate of the nutrients. This equation applies to the entire microchannel as full cell seeding coverage is assumed.

Boundary and initial conditions are described as follows:

- equation 3 is valid at the boundary between the top of first layer microchannels and medium for $D_A=D_2$ and $D_B=D_1$ and for the boundary between the bottom of the microchannels and inner-porosity of the sheets for $D_A=D_2$ and $D_B=D_3$; describing flux continuity over the respective boundaries
- equation 4 is valid as initial condition; representing nutrient concentrations of fresh medium present in the scaffold at the start of the experiment

Inner-Porosity of Scaffold Sheets (Domain 3)

$$\varepsilon\frac{\partial c}{\partial t}=D_3\left(\frac{\partial c}{\partial x}+\frac{\partial c}{\partial y}\right) \tag{7}$$

with ε = porosity. Nutrients are only present in the pores of the sheets inner-part; the porosity term expresses a concentration gradient that develops in time over the scaffold inner-porosity due to nutrient consumption by the cells.

Boundary and initial conditions are described as follows:

- equation 2 is valid at all exterior boundaries, except the top boundary, and all interior boundaries connecting inner-parts of stacked scaffold sheets; describing symmetry of microchannels and scaffold inner-parts for the stacked layers

- equation 3 is valid at the boundary between the top of first layer microchannel ridges and medium for $D_A = D_3$ and $D_B = D_1$ and for the boundary between sheet inner porosity and microchannels for $D_A = D_3$ and $D_B = D_2$; describing flux continuity over the respective boundaries
- equation 4 is valid as initial condition; representing nutrient concentrations of fresh medium present in the scaffold at the start of the experiment

Dynamic Culturing

With the introduction of flow of cell culture medium, the system enters the fluidic regime combined with mass transfer of nutrients. Although scaffold sheets, including micropattern, are about 90 μm in thickness; well-known macro-scale transport equations can be applied since for these scaffold sizes the same transport phenomena are still dominant.[25,26]

A pseudo 3D mode was used to model nutrient concentrations over perfused multi-layer scaffolds bringing about replacement of the space variable along the direction of the flow in time. Therefore, with a given velocity, an increment in time stands for a displacement in the direction of the flow. This pseudo 3D mode can be applied when the following requirements are satisfied:

- the model is defined steady-state; no accumulation of nutrients occurs in time and cell proliferation is not modelled directly but indirectly through prediction for distinct cell densities
- convection is constant and dominating solely in one direction; full developed laminar flow is present in the microchannels and does not change over the length of the microchannel
- in the direction of the flow, diffusion is negligible
- in the flow direction the geometry is the same/constant;

Since the designed model meets all requirements, the use of the pseudo3D mode was valid. Based on these assumptions, the convection-diffusion equation can be written in following form:

$$u_{dl}\frac{\partial c}{\partial t} + \nabla \cdot (-D\nabla c) = R \tag{8}$$

with u_{dl} a variable of interest as function of x and where R is as described in Equation 6.

The Navier-Stokes equation for laminar flow of incompressible fluids is used to describe nutrient flow in microchannels of scaffold sheets; with the channels considered rectangular tubes:[27]

$$u_{dl} = \frac{u_{channel}}{\langle u_{channel}\rangle} = 2 \cdot \left(16 \cdot \frac{(x_1 - x)\cdot(x - x_0)}{(x_1 - x_0)^2} \cdot \frac{(y_1 - y)\cdot(y - y_0)}{(y_1 - y_0)^2}\right) \tag{9}$$

Where x stands for the width of one symmetry element, i.e. from one ridge of the microchannel to the next ridge; and y stands for the height of one symmetry element, i.e. from the bottom of the microchannel to the top of the ridges (see also Figure 2c).

Under dynamic culture conditions two domains can be distinguished: cell seeded microchannels where perfusion occurs and sheet inner-porosity. To solve the model; these two domains were considered separately with respect to equations, boundary- and initial conditions.

Cell Seeded Microchannels

$$u_{dl}\frac{\partial c}{\partial t} - D_2\left(\frac{\partial^2 c}{\partial x^2} + \frac{\partial^2 c}{\partial y^2}\right) = R \tag{10}$$

Boundary and initial conditions are described as follows:

- Equation 2 is valid at $(x,y) = (\frac{1}{2}(x_1 - x_0), \frac{1}{2}(y_1 - y_0))$; represents symmetry of the concentration gradient at the centre of microchannels
- Equation 3 is valid at interior boundaries for $D_A = D_2$ and $D_B = D_3$ and at $y = 0$ and $y = y_1$; describing flux continuity over boundaries between microchannels and inner-porosity of stacked sheets

- Equation 4 is valid as initial condition; representing nutrient concentrations of fresh medium at the inlet of microchannels.

Inner-Porosity of Scaffold Sheets

$$D_3\left(\frac{\partial^2 c}{\partial x^2}+\frac{\partial^2 c}{\partial y^2}\right)=0 \quad (11)$$

Boundary and initial conditions are described as follows:

- Equation 2 is valid at all exterior boundaries, except $y = y_1$; represents symmetry of microchannels
- Equation 3 is valid at interior boundaries for $D_A = D_3$ and $D_B = D_2$ and at $y = 0$ and $y = y_1$; describing flux continuity over boundaries connecting inner-porosity of stacked sheets with microchannels
- Equation 4 is valid as initial condition with $c_0 = 0$; representing no flow of medium into the inner-porosity of sheets at the inlet as well as absence of medium in the inner-porosity at the start of the experiment in this specific case.

Results and Discussion

Static Conditions

Figure 3a and 3b present model predictions for glucose and oxygen concentrations, respectively, for 48 hours of culture under static conditions. For these predictions, we assume transport only originates from and to medium present on top. The y-axis displays nutrient concentration (C) normalised over the initial value (C_0), whereas the x-axis displays height within the scaffold (H) normalized over the total scaffold height (H_0). Therefore, value 1 on y-axis represents the initial nutrient value, whereas on x-axis value 1 represents the top of the scaffold and 0 the bottom. In case of the 5-layer scaffold, 1 on the x-axis indicates the top of layer 1, 0.8 the top of layer 2, ..., and 0.2 the top of layer 5. 'Black' symbols represent a cell number of $2 \cdot 10^{12}$ cells/m^3, equal to seeding density. 'Grey' symbols represent a cell number of $3 \cdot 10^{13}$ cells/m^3, corresponding to high confluence per layer in line with culturing for at least 4 days or more. The graphs show nutrient concentration gradients in case of 1 layer (control) and 5 stacked sheet layers.

At lower cell density (black symbols), the model predicts no nutrient deficiency within 48 hours of culturing for both model nutrients; i.e. glucose and oxygen, see Figure 3a, 3b respectively. In both cases, the cells on 5-layer scaffolds consume significantly more compared to a single layer as expected due to higher cell number in total. These predictions indicate refreshing medium after 2 days would be sufficient at low cell densities. Since nutrients are still at 50% or more of their initial values, extrapolating this refreshing rate to the first days of culturing experiments seems valid even though cell number will increase (not considered by the model). For cell density corresponding to high confluence levels (grey symbols), the model predicts significantly higher nutrient consumption and eventually nutrient depletion within 48 hours for the 5-layer scaffolds. In fact, the model predicts complete consumption of glucose (Figure 3a), whereas depletion of oxygen occurs only between the 2nd and 3rd layer due to replenished oxygen levels into the bulk medium by diffusion from air (Figure 3b). For one single sheet nutrients are predicted to be just sufficient although glucose levels are less than 20% of its initial value and almost zero close to the cell layer.

Refreshing medium more often or increasing medium volume will most likely improve these results; however, it may not be sufficient. At some point in time diffusion towards lower layers will not be able to keep in pace with consumption by the increased number of cells, independent of nutrient concentration in the bulk medium. As a result nutrient depletion will occur. This trend is also seen for oxygen in the 5-layer scaffolds. Dynamic culturing would improve transport of nutrients towards inner layers as the channels provide space throughout the complete scaffold for medium perfusion.

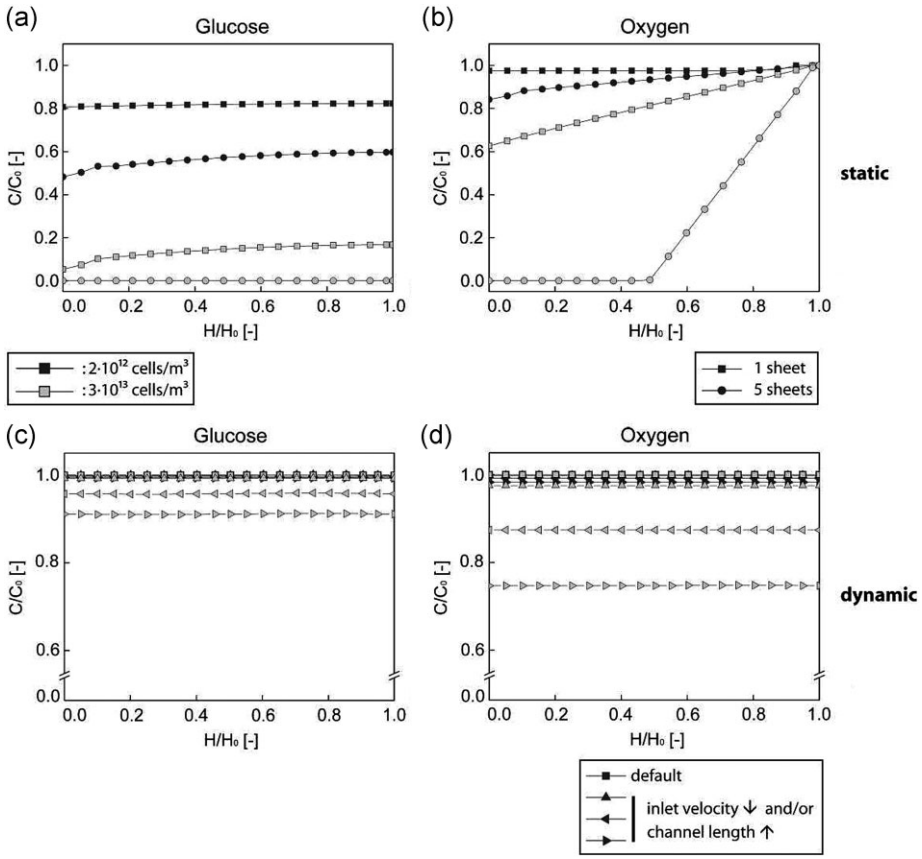

Figure 3.
Modeling of (a, c) glucose and (b, d) oxygen levels through multi-layer scaffolds for various cell densities at day 2 under (a, b) static and (c, d) dynamic conditions.

Dynamic Conditions

The model predicts culturing scaffolds under dynamic conditions, i.e., introducing medium flow through channels, improves glucose and oxygen availability per layer; see Figure 3c and 3d, respectively. Nutrient concentrations for each layer are predicted to be sufficient in all situations indicating dynamic culturing conditions improve nutrient availability already under mild flow conditions.

For these predictions, each layer was considered equal since convective transport through channels was considered dominant neglecting diffusive transport. Nutrient concentration varied as function of medium residence time, which amongst others is influenced by the length of the channel and inlet-flow of the medium. Variation with channel length is directly correlated to the inlet flow of medium; both increased channel length and decreased inlet flow would prolong residence time. In the calculations, residence times representing experimental relevant conditions up to 10x default values are included. Increase in residence time of 10× implies increase in channel length of 10x (i.e. 30 cm), decrease in flow inlet velocity of 10× (i.e. $7.5 \cdot 10^{-4}$ m/s) or combined partial contribution of both. As can be appreciated from Figure 3c and 3d, even for the longest residence time (10× default value) glucose and oxygen levels are predicted to be around 90 and 75% of their initial values, respectively.

Comparison to Experimental Results

The above modelling predictions are consistent with experimental results reported earlier.[15] There, DNA analysis of scaffolds cultured statically for 7 days showed that all layers have lower proliferation compared to the single layer, including the outer layer; supporting the hypothesis discussed in our earlier work that cells on inner layers inhibit cell proliferation on the outer layer. Cell number was also found dramatically lower in 3rd and 4th layers consistent with our predictions of low oxygen and glucose levels for these layers. Scaffolds cultured under dynamic conditions revealed about doubled DNA concentrations or more compared to scaffolds under static conditions; all inner layers had DNA concentrations comparable to the control single layer with all cells in direct contact with medium. The 1st layer which is in direct contact with medium still has the highest DNA values.[15]

Conclusion

The numerical model presented here enables good prediction of nutrient supply through multilayer scaffolds and therefore can be used for designing of optimal multilayer scaffolds for TE. In the future more complex cell-material and cell-cell interactions, and how these interactions affect nutrient supply throughout the scaffold as well as various scaffold designs could be included in the model. In fact, improved understanding of nutrient and oxygen supply through 3D scaffolds can be gained using this model leading to design and construction of 3D scaffolds supporting uniform cell growth.

Nomenclature Model

X_0	Initial value X
X_1	Value X at domain 1: medium
X_2	Value X at domain 2: cell-seeded microchannel
X_3	Value X at domain 3: inner-porosity scaffold sheet
c	Nutrient concentration
d	Cell seeding density
D	Nutrient diffusion coefficient
R	Zero-order consumption rate of nutrients ($V \cdot d$)
t	Time
u_{dl}	variable
V	Consumption rate per cell

Acknowledgements: B.J. Papenburg and D. Stamatialis acknowledge the Spearhead program: 'Advanced Polymeric Microstructures for Tissue Engineering' of the University of Twente (MIRA, Institute for Biomedical Engineering and Technical Medicine) for financial support.

[1] R. Langer, J. P. Vacanti, *Science* **1993**, *260*, 920.
[2] J. C. Y. Dunn, W.-Y. Chan, V. Cristini, J. S. Kim, J. Lowengrub, S. Singh, B. M. Wu, *Tissue Engineering* **2006**, *12*, 705.
[3] H. C. H. Ko, B. K. Milthorpe, C. D. McFarland, *Eur. Cells Mater.* **2007**, *14*, 1.
[4] J. Malda, T. J. Klein, Z. Upton, *Tissue Engineering* **2007**, *13*, 2153.
[5] J. Malda, J. Rouwkema, D. E. Martens, E. P. le Comte, F. K. Kooy, J. Tramper, C. A. van Blitterswijk, J. Riesle, *Biotechnol. Bioeng.* **2004**, *86*, 9.
[6] R. Pörtner, S. Nagel-Heyer, C. Goepfert, P. Adamietz, N. M. Meenen, *Journal of Bioscience and Bioengineering* **2005**, *100*, 235.
[7] I. Martin, D. Wendt, M. Heberer, *Trends in Biotechnology* **2004**, *22*, 80.
[8] Y. Martin, P. Vermette, *Biomaterials* **2005**, *26*, 7481.
[9] V. Barron, E. Lyons, C. Stenson-Cox, P. E. McHugh, A. Pandit, *Ann. Biomed. Eng.* **2003**, *31*, 1017.
[10] R. Dennis, B. Smith, A. Philp, K. Donnelly, K. Baar, "Bioreactors for Guiding Muscle Tissue Growth and Development" in: *Bioreactor Systems for Tissue Engineering*, **2009**, p. 39.
[11] H. Mertsching, J. Hansmann, "Bioreactor Technology in Cardiovascular Tissue Engineering", in *Bioreactor Systems for Tissue Engineering*, **2009**, p. 29.
[12] R. J. Whittaker, R. Booth, R. Dyson, C. Bailey, L. Parsons Chini, S. Naire, S. Payvandi, Z. Rong, H. Woollard, L. J. Cummings, S. L. Waters, L. Mawasse, J. B. Chaudhuri, M. J. Ellis, V. Michael, N. J. Kuiper, S. Cartmell, *Journal of Theoretical Biology* **2009**, *256*, 533.
[13] H. Ye, D. B. Das, J. T. Triffitt, Z. Cui, *Journal of Membrane Science* **2006**, *272*, 169.
[14] H. Ye, Z. Xia, D. Ferguson, J. Triffitt, Z. Cui, *Journal of Materials Science: Materials in Medicine* **2007**, *18*, 641.

[15] B. J. Papenburg, J. Liu, G. A. Higuera, A. M. C. Barradas, J. de Boer, C. A. van Blitterswijk, M. Wessling, D. Stamatialis, *Biomaterials* **2009**, *30*, 6228.
[16] B. J. Papenburg, L. Vogelaar, L. A. M. Bolhuis-Versteeg, R. G. H. Lammertink, D. Stamatialis, M. Wessling, *Biomaterials* **2007**, *28*, 1998.
[17] D. F. Stamatialis, B. J. Papenburg, M. Gironés, S. Saiful, S. N. M. Bettahalli, S. Schmitmeier, M. Wessling, *Journal of Membrane Science* **2008**, *308*, 1.
[18] N. S. Abdullah, D. B. Das, H. Ye, Z. F. Cui, *International Journal of Artificial Organs* **2006**, *29*, 841.
[19] F. Coletti, S. Macchietto, N. Elvassore, *Industrial & Engineering Chemistry Research* **2006**, *45*, 8158.
[20] B. G. Sengers, C. C. van Donkelaar, C. W. J. Oomens, F. P. T. Baaijens, *Biotechnology Progress* **2005**, *21*, 1252.
[21] H. Ye, D. B. Das, J. T. Triffitt, Z. F. Cui, *Journal of Membrane Science* **2006**, *272*, 169.
[22] W. M. Saltzman, "*Tissue Engineering: principles for the design of replacement organs and tissues*", 1st edition, Oxford University Press, Oxford **2004**.
[23] E. Figallo, C. Cannizzaro, S. Gerecht, J. A. Burdick, R. Langer, N. Elvassore, G. Vunjak-Novakovic, *Lab on a chip* **2007**, *7*, 710.
[24] M. C. Lewis, B. D. MacArthur, J. Malda, G. Pettet, C. P. Please, *Biotechnol. Bioeng.* **2005**, *91*, 607.
[25] V. Hessel, S. Hardt, H. Loewe, "*Chemical Micro Process Engineering: Fundamentals, Modelling and reactions*", Wiley-VCH, Weinheim **2004**.
[26] P. Tabeling, S. Cheng, "*Introduction to Microfluidics*", Cambridge University Press, New York **2005**.
[27] COMSOL, "*Manuals COMSOL 3.2 and 3.3*", 2005–2007.

